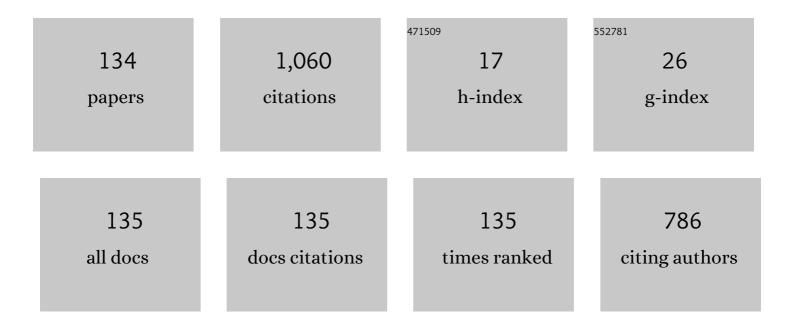
## Zhen-Sen Wu

List of Publications by Year in descending order

Source: https://exaly.com/author-pdf/8786620/publications.pdf Version: 2024-02-01



#	Article	IF	CITATIONS
1	Analysis of the radiation force and torque exerted on a chiral sphere by a Gaussian beam. Optics Express, 2013, 21, 8677.	3.4	51
2	Potential Effects of the Ionosphere on Space-Based SAR Imaging. IEEE Transactions on Antennas and Propagation, 2008, 56, 1968-1975.	5.1	44
3	Generation of multiple beams carrying different orbital angular momentum modes based on anisotropic holographic metasurfaces in the radio-frequency domain. Applied Physics Letters, 2019, 114, .	3.3	41
4	Calculation of electromagnetic scattering by a large chiral sphere. Applied Optics, 2012, 51, 6661.	1.8	38
5	Millimeter-Wave Attenuation Due to Fog and Clouds. Journal of Infrared, Millimeter and Terahertz Waves, 2000, 21, 1607-1615.	0.6	34
6	AN IMPROVED TWO-SCALE MODEL WITH VOLUME SCATTERING FOR THE DYNAMIC OCEAN SURFACE. Progress in Electromagnetics Research, 2009, 89, 39-56.	4.4	31
7	Electromagnetic scattering for a uniaxial anisotropic sphere in an off-axis obliquely incident Gaussian beam. Journal of the Optical Society of America A: Optics and Image Science, and Vision, 2010, 27, 1457.	1.5	31
8	Light scattering of a Laguerre–Gaussian vortex beam by a chiral sphere. Journal of the Optical Society of America A: Optics and Image Science, and Vision, 2016, 33, 475.	1.5	31
9	GPS total electron content and surface latent heat flux variations before the 11 March 2011 M9.0 Sendai earthquake. Advances in Space Research, 2011, 48, 1311-1317.	2.6	30
10	Anomalous enhancement of electric field derived from ionosonde data before the great Wenchuan earthquake. Advances in Space Research, 2011, 47, 1001-1005.	2.6	27
11	A New Rain Attenuation Prediction Model for the Earth-Space Links. IEEE Transactions on Antennas and Propagation, 2018, 66, 5432-5442.	5.1	25
12	STUDY ON SCINTILLATION CONSIDERING INNER- AND OUTER-SCALES FOR LASER BEAM PROPAGATION ON THE SLANT PATH THROUGH THE ATMOSPHERIC TURBULENCE. Progress in Electromagnetics Research, 2008, 80, 277-293.	4.4	23
13	Parallel Computation of Aerial Target Reflection of Background Infrared Radiation: Performance Comparison of OpenMP, OpenACC, and CUDA Implementations. IEEE Journal of Selected Topics in Applied Earth Observations and Remote Sensing, 2016, 9, 1653-1662.	4.9	22
14	Research on Sea Clutter Reflectivity Using Deep Learning Model in Industry 4.0. IEEE Transactions on Industrial Informatics, 2020, 16, 5929-5937.	11.3	22
15	GPU-Accelerated Computation for Electromagnetic Scattering of a Double-Layer Vegetation Model. IEEE Journal of Selected Topics in Applied Earth Observations and Remote Sensing, 2013, 6, 1799-1806.	4.9	21
16	A temporal threeâ€dimensional simulation of samarium release in the ionosphere. Journal of Geophysical Research: Space Physics, 2016, 121, 10,508.	2.4	20
17	Statistical temporal behaviour of pulse wave propagation through continuous random media. Waves in Random and Complex Media, 2003, 13, 59-73.	1.5	19
18	Study on the Prediction of Troposcatter Transmission Loss. IEEE Transactions on Antennas and Propagation, 2016, 64, 1071-1079.	5.1	19

#	Article	IF	CITATIONS
19	Analytic Specific Attenuation Model for Rain for Use in Prediction Methods. Journal of Infrared, Millimeter and Terahertz Waves, 2001, 22, 113-120.	0.6	18
20	Design of Multiple-Polarization Reflectarray for Orbital Angular Momentum Wave in Radio Frequency. IEEE Antennas and Wireless Propagation Letters, 2018, 17, 2269-2273.	4.0	18
21	Solution for the Fourth Moment Equation of Waves in Random Continuum Under Strong Fluctuations: General Theory and Plane Wave Solution. IEEE Transactions on Antennas and Propagation, 2007, 55, 1613-1621.	5.1	17
22	Solar cycle variation of the monthly median foF2 at Chongqing station, China. Advances in Space Research, 2008, 42, 213-218.	2.6	17
23	An efficient spatial deblocking of images with DCT compression. , 2015, 42, 80-88.		17
24	Scattering of a partially coherent Gaussian–Schell beam from a diffuse target in slant atmospheric turbulence. Journal of the Optical Society of America A: Optics and Image Science, and Vision, 2011, 28, 1531.	1.5	16
25	Sea Clutter Amplitude Prediction Using a Long Short-Term Memory Neural Network. Remote Sensing, 2019, 11, 2826.	4.0	16
26	HIGH RESOLUTION RANGE PROFILE IDENTIFYING SIMULATION OF LASER RADAR BASED ON PULSE BEAM SCATTERING CHARACTERISTICS OF TARGETS. Progress in Electromagnetics Research, 2009, 96, 193-204.	4.4	15
27	Scattering from a multilayered chiral sphere using an iterative method. Journal of Quantitative Spectroscopy and Radiative Transfer, 2016, 173, 72-82.	2.3	15
28	Bilateral Filtering and Directional Differentiation for Bayer Demosaicking. IEEE Sensors Journal, 2017, 17, 726-734.	4.7	14
29	Parallel Computation of EM Backscattering from Large Three-Dimensional Sea Surface with CUDA. Sensors, 2018, 18, 3656.	3.8	14
30	GPU-Accelerated Computation of Time-Evolving Electromagnetic Backscattering Field From Large Dynamic Sea Surfaces. IEEE Transactions on Industrial Informatics, 2020, 16, 3187-3197.	11.3	14
31	Forecasting the ionospheric f0F2 parameter one hour ahead using a support vector machine technique. Journal of Atmospheric and Solar-Terrestrial Physics, 2010, 72, 1341-1347.	1.6	12
32	Analysis of rainbow scattering by a chiral sphere. Optics Express, 2013, 21, 21879.	3.4	12
33	Inversion Method of Regional Range-Dependent Surface Ducts with a Base Layer by Doppler Weather Radar Echoes Based on WRF Model. Atmosphere, 2020, 11, 754.	2.3	12
34	Electromagnetic Scattering from Deterministic Sea Surface With Oceanic Internal Waves via the Variable-Coefficient Gardener Model. IEEE Journal of Selected Topics in Applied Earth Observations and Remote Sensing, 2018, 11, 355-366.	4.9	11
35	Reflection, Transmission, and Absorption of Vortex Beams Propagation in an Inhomogeneous Magnetized Plasma Slab. IEEE Transactions on Antennas and Propagation, 2018, 66, 4194-4201.	5.1	11
36	Bayesian method application for color demosaicking. Optical Engineering, 2018, 57, 1.	1.0	11

#	Article	IF	CITATIONS
37	Statistical characteristics of a Gaussian beam reflected by a retro-reflector in atmospheric turbulence. Optik, 2018, 158, 1361-1369.	2.9	10
38	POLARIZATION CHARACTERISTICS OF A PARTIALLY COHERENT GAUSSIAN SCHELL-MODEL BEAM IN SLANT ATMOSPHERIC TURBULENCE. Progress in Electromagnetics Research, 2011, 121, 453-468.	4.4	9
39	Scattering and propagation of a Laguerre–Gaussian vortex beam by uniaxial anisotropic bispheres. Journal of Quantitative Spectroscopy and Radiative Transfer, 2018, 209, 1-9.	2.3	9
40	GPU-Accelerated Massively Parallel Computation of Electromagnetic Scattering of a Time-Evolving Oceanic Surface Model I: Time-Evolving Oceanic Surface Generation. IEEE Journal of Selected Topics in Applied Earth Observations and Remote Sensing, 2018, 11, 2752-2762.	4.9	9
41	Improvements for scattering from a large-sized chiral cylinder at an oblique incidence. Journal of Quantitative Spectroscopy and Radiative Transfer, 2015, 162, 50-55.	2.3	8
42	A Model of Telecommunication Network Performance Anomaly Detection Based on Service Features Clustering. IEEE Access, 2017, 5, 17589-17596.	4.2	8
43	Filter-based Bayer Pattern CFA Demosaicking. Circuits, Systems, and Signal Processing, 2017, 36, 2917-2940.	2.0	8
44	Effect of nanoscale roughness on optical trapping properties of surface plasmon polaritons exerted on nanoparticle. Journal of Quantitative Spectroscopy and Radiative Transfer, 2018, 219, 339-349.	2.3	8
45	Numerical simulation for echo characteristics of laser beams reflected by retro-reflectors in atmospheric turbulence. Optik, 2019, 179, 244-251.	2.9	8
46	Scattering of Electromagnetic Waves With Orbital Angular Momentum on Metallic Sphere. IEEE Antennas and Wireless Propagation Letters, 2020, 19, 1365-1369.	4.0	8
47	Multiscale Decomposition Prediction of Propagation Loss in Oceanic Tropospheric Ducts. Remote Sensing, 2021, 13, 1173.	4.0	8
48	Method of Calculating the Radiance of Point-Source Target in Infrared Image. Journal of Infrared, Millimeter and Terahertz Waves, 2002, 23, 1347-1355.	0.6	7
49	Second-order statistics of radio wave propagation through the structured ionosphere. Journal of Atmospheric and Solar-Terrestrial Physics, 2004, 66, 971-980.	1.6	7
50	Scattering of an anisotropic sphere by an arbitrarily incident Hermite–Gaussian beam. Journal of Quantitative Spectroscopy and Radiative Transfer, 2016, 170, 117-130.	2.3	7
51	Determination of the complex refractivity of Au, Cu and Al in terahertz and far-infrared regions from reflection spectra measurements. Infrared Physics and Technology, 2017, 80, 58-64.	2.9	7
52	Propagation of arbitrarily polarized terahertz Bessel vortex beam in inhomogeneous unmagnetized plasma slab. Physics of Plasmas, 2018, 25, 123505.	1.9	7
53	Performance comparison of GA, PSO, and DE approaches in estimating low atmospheric refractivity profiles. Wuhan University Journal of Natural Sciences, 2010, 15, 433-439.	0.4	6
54	Propagation Characteristics of Oblique Incident Terahertz Wave in Nonuniform Dusty Plasma. International Journal of Antennas and Propagation, 2016, 2016, 1-6.	1.2	6

#	Article	IF	CITATIONS
55	Study on the maximum calculation height and the maximum propagation angle of the troposcatter wideâ€angle parabolic equation method. IET Microwaves, Antennas and Propagation, 2016, 10, 686-691.	1.4	6
56	Ionospheric effects on repeat-pass SAR interferometry. Advances in Space Research, 2017, 60, 1504-1515.	2.6	6
57	Research on anomaly detection algorithm based on generalization latency of telecommunication network. Future Generation Computer Systems, 2018, 85, 9-18.	7.5	6
58	Simulation of full-polarization electromagnetic backscattering characteristics of large number of high-density chaff clouds. , 2019, , .		6
59	Propagation of a terahertz Bessel vortex beam through a homogeneous magnetized plasma slab. Waves in Random and Complex Media, 2022, 32, 1535-1550.	2.7	6
60	Optical Binding Force between Two Chiral Spheres by an Incident On-axis Gaussian Beam. Procedia Engineering, 2015, 102, 329-335.	1.2	5
61	Retrieval Method for Complex Refractivity From Reflection Measurements of Rough Surfaces. IEEE Antennas and Wireless Propagation Letters, 2017, 16, 1581-1584.	4.0	5
62	Evolution of linear edge dislocation in atmospheric turbulence and free space. Journal of Modern Optics, 2019, 66, 17-25.	1.3	5
63	Speckle statistical properties of Gaussian beam from a semi-rough target in the atmospheric turbulence. Optik, 2013, 124, 6760-6764.	2.9	4
64	Analysis on the Distribution of Random Rough Surface Scattering by Monte-Carlo Method. , 2018, , .		4
65	OAM crosstalk of multiple coaxial THz vortex beams propagating through an inhomogeneous unmagnetized plasma slab. Physics of Plasmas, 2019, 26, .	1.9	4
66	Deep learning for inversion of significant wave height based on actual sea surface backscattering coefficient model. Multimedia Tools and Applications, 2020, 79, 34173-34193.	3.9	4
67	Integrated Physical Optics for Calculating Electric-Large Metallic Sphere Scattering Irradiated by Vortex Wave in Microwave Frequency Band. IEEE Antennas and Wireless Propagation Letters, 2022, 21, 1288-1292.	4.0	4
68	Statistical Study of Ionospheric Equivalent Slab Thickness at Guam Magnetic Equatorial Location. Remote Sensing, 2021, 13, 5175.	4.0	4
69	Effect of window function on absorbing layers top boundary in parabolic equation. , 2014, , .		3
70	Backscatter amplification effect for a reflected partially coherent Gaussian beam in turbulent medium. Journal of Quantitative Spectroscopy and Radiative Transfer, 2015, 163, 1-6.	2.3	3
71	Analysis of the Co-channel Interference caused by Atmospheric Duct and Tropospheric scattering. , 2018, , .		3
72	Modified model of equivalent height for predicting atmospheric attenuation at frequencies below 350 GHz. IET Microwaves, Antennas and Propagation, 2018, 12, 1420-1427.	1.4	3

Zhen-Sen Wu

#	Article	IF	CITATIONS
73	Parallel BRDF-based infrared radiation simulation of aerial targets implemented on Intel Xeon processor and Xeon Phi coprocessor. Journal of Real-Time Image Processing, 2019, 16, 49-60.	3.5	3
74	Time delay of ionospheric TEC storms to geomagnetic storms and pre-storm disturbance events in East Asia. Advances in Space Research, 2021, 67, 1535-1545.	2.6	3
75	Thomson scattering of a vector Bessel vortex beam by a non-relativistic electron. Physics of Plasmas, 2021, 28, .	1.9	3
76	Simulating the Scattering Echo and Inverse Synthetic Aperture Lidar Imaging of Rough Targets. Annalen Der Physik, 0, , 2100491.	2.4	3
77	Scattering of a general partially coherent beam from a diffuse target in atmospheric turbulence. Chinese Physics B, 2014, 23, 094202.	1.4	2
78	Study on the scale relation of electromagnetic scattering from perfectly conducting target. , 2014, , .		2
79	A study of electromagnetic scattering from sea surface with breaking waves using generalized forward-backward method. , 2016, , .		2
80	Experimental study on surface scattering characteristics of wall and ground in the millimeter wave. , 2018, , .		2
81	Features of X-Band Radar Backscattering Simulation Based on the Ocean Environmental Parameters in China Offshore Seas. Sensors, 2018, 18, 2450.	3.8	2
82	THz Scattering Characteristics of Simple Body. , 2019, , .		2
83	Statistical study of the time delay of ionospheric TEC storms to geomagnetic storms in Taoyuan, Taiwan. Advances in Space Research, 2020, 65, 86-94.	2.6	2
84	Stability and dynamics of chiral nanoparticles in lateral optical binding induced by high-order Bessel beams. Journal of Quantitative Spectroscopy and Radiative Transfer, 2020, 243, 106824.	2.3	2
85	Researching on the Deterministic Channel Models for Urban Microcells Considering Diffraction Effects. Energies, 2021, 14, 2143.	3.1	2
86	GPU-Accelerated Computation of EM Scattering of a Time-Evolving Oceanic Surface Model II: EM Scattering of Actual Oceanic Surface. Remote Sensing, 2022, 14, 2727.	4.0	2
87	High-efficiency numerical computing in low-grazing scattering from sea surface using resistive tapering and forward-backward method. , 2014, , .		1
88	Statistic of a Gaussian beam from an arbitrary rough target in the single passage atmospheric turbulence. Science China: Physics, Mechanics and Astronomy, 2014, 57, 1854-1859.	5.1	1
89	Theoretical model and experimental study of beam scattering from ocean surface. , 2014, , .		1
90	Superresolution of Hyperspectral Image Using Advanced Nonlocal Means Filter and Iterative Back Projection. Journal of Sensors, 2015, 2015, 1-5.	1.1	1

#	Article	IF	CITATIONS
91	Electromagnetic scattering for multilayered spheres induced by laser sheet beam. , 2016, , .		1
92	Difference field scattering properties between inlaid redundant particles and slightly rough optical surface. , 2016, , .		1
93	Scattering of a uniaxial anisotropic sphere incident by a Laguerre-Gaussian vortex beam. , 2016, , .		1
94	Numerical simulation of abnormal incoherent scatter spectra based on Zakharov model. , 2016, , .		1
95	The Big Data Processing of HF Sky-Wave Radar Sea Echo for Detection of Sea Moving Targets. International Journal of Information Technology and Web Engineering, 2017, 12, 56-71.	1.6	1
96	Study of infrared reflection characteristics of aerial target using MODIS data on GPU. Journal of Real-Time Image Processing, 2018, 15, 643-655.	3.5	1
97	Scattering of Plane Waves From an Infinite Dielectric Periodic Surface. Radio Science, 2019, 54, 758-769.	1.6	1
98	Scattering of a Gaussian beam by an anisotropically coated circular cylinder. Waves in Random and Complex Media, 2019, 29, 54-62.	2.7	1
99	Measurement and analysis of the scattering properties of cement surfaces of urban environment in the millimeter waveband. Transactions on Emerging Telecommunications Technologies, 0, , e4251.	3.9	1
100	Inversion for Inhomogeneous Surface Duct without a Base Layer Based on Ocean-Scattered Low-Elevation BDS Signals. Remote Sensing, 2021, 13, 3914.	4.0	1
101	Synthesis and Characterization of Three Diverse Coordination Frameworks under Coâ€ligand Intervention. Chinese Journal of Chemistry, 2009, 27, 317-323.	4.9	0
102	Accelerating the Calculation of Scattering of Complex Targets from Background Radiation with CUDA, OpenACC and OpenHMPP. , 2013, , .		0
103	The Brewster angel effect for backscattering analysis of sea spike at a low grazing angle. , 2014, , .		0
104	Two-frequency mutual coherence function of UV pulses in soot aerosols. , 2014, , .		0
105	A study of composite electromagnetic scattering from rough sea surface and missile-like target basing on the efficient numerical algorithm. , 2014, , .		0
106	Inversion of ground parameters using genetic algorithms and engineering modeling for bistaticscattering. , 2014, , .		0
107	The application of PE in the propagation of VLF wave in earth-ionosphere waveguide. , 2014, , .		0
108	Characteristics of aerial targets under Earth-atmosphere environment in visible band based on MODIS data. , 2014, , .		0

#	Article	IF	CITATIONS
109	Analysis of abnormally enhanced ion line power spectra structure in ionospheric heating experiments. , 2014, , .		0
110	The analysis of double-peaked spectrum in the enhanced plasma lines. , 2014, , .		0
111	Scattering of Plasma Anisotropic Spherical Particle Incident by a High-order Bessel Beam. Procedia Engineering, 2015, 102, 167-173.	1.2	0
112	Analysis and study on the prediction model of rain attenuation in short path. , 2016, , .		0
113	Statistical analysis of signatures and contributing factors of atmospheric ducts based on the sounding data. , 2016, , .		0
114	Low latitude ionospheric tomography based on the multi-station method. , 2016, , .		0
115	The analysis on Doppler spectrum of 2-D sea clutter in multi-band. , 2016, , .		0
116	The study of the rough medium surface by improved IPO. , 2016, , .		0
117	Transmission Characteristics of Polarized Light in Low Visibility Fog. , 2018, , .		0
118	Study of spatial characteristics of artificial field aligned scattering. , 2018, , .		0
119	Numerical Simulation of Scattering from an Infinite Dielectric Periodic Surface. , 2018, , .		0
120	Difference Scattering Field Properties between Multilayered Defect Particles and Slightly Rough Optical Surface. , 2018, , .		0
121	Distortion of Polarized Bessel Vortex Beams Propagation in Sandstorm. , 2018, , .		0
122	Paraxial Propagation of the Second-order Airy Vortex Beams in the Free Space. , 2018, , .		0
123	Laser Attenuation Model in Low Visibility Fog. , 2019, , .		0
124	A Central Symmetrical and Low-Profile Omnidirectional Circularly Polarized Antenna. International Journal of Antennas and Propagation, 2019, 2019, 1-12.	1.2	0
125	Scattering from a multilayered chiral sphere: Internal and near fields. Journal of Quantitative Spectroscopy and Radiative Transfer, 2019, 232, 156-164.	2.3	0
126	THz wave background radiation at upper troposphere. Multimedia Tools and Applications, 2020, 79, 8767-8780.	3.9	0

#	Article	IF	CITATIONS
127	Vector Rayleigh Diffraction of High-Power Laser Diode Beam in Optical Communication. International Journal of Optics, 2020, 2020, 1-7.	1.4	Ο
128	Scattering of a Gaussian beam by an anisotropic-coated eccentric conducting circular cylinder. International Journal of Microwave and Wireless Technologies, 2020, 12, 900-905.	1.9	0
129	Simulation of Spatiotemporal Variation of Evaporation Duct Height based on WRF Model with Experimental Validation. , 2021, , .		0
130	Study on 340 GHz Wave Scintillation Characteristics Based on Experimental Data. , 2021, , .		0
131	Behavior from Phase Factor Approximate Upon the Beam Propagation in Bessel Beam Angular Spectrum Expansion. , 2021, , .		Ο
132	Study on the Scattering Coefficients of the Cement Surface at 28GHz. , 2021, , .		0
133	Inverse Synthetic Aperture LiDAR Imaging of Rough Targets under Small Rotation Angles. Remote Sensing, 2022, 14, 2694.	4.0	Ο
134	Phase Turbulence Prediction Method for Line-of-Sight Multiple-Input–Multiple-Output Links Caused by Atmospheric Environment. IEEE Antennas and Wireless Propagation Letters, 2022, 21, 1867-1871.	4.0	0